

Developing improved tissue-engineered buccal mucosa grafts for urethral reconstruction

Abdulmuttalip Simsek^{1,2}; Anthony J. Bullock, MD²; Sabi Roman, MD²; Chirstoper R. Chapple, MD¹; Sheila MacNeil, MD²

¹Royal Hallamshire Hospital, Department of Female and Reconstructive Urology, Sheffield; ²University of Sheffield, Department of Materials Science & Engineering, Sheffield; United Kingdom

Cite as: *Can Urol Assoc J* 2018;12(5):E234-42 <http://dx.doi.org/10.5489/cuaj.4826>

Published online February 6, 2018

Abstract

Introduction: We aimed to compare alternative synthetic scaffolds suitable for future implantation and to examine the use of an inhibitor of lysyl oxidase (beta-amino-propionitrile [β -APN]) to reduce contraction in these implants.

Methods: Three synthetic scaffolds were compared to natural dermis as substrates for the production of tissue-engineered skin. For natural dermis, Euroskin was used to provide a cell-free cadaveric dermis. Synthetic scaffolds consisted of microfibrillar poly-L-lactic acid (PLA), nanofibrillar poly(3-hydroxybutyrate-co-3-hydroxyvalerate) (PHBV), and a micro-/nanofibrillar trilayer of PLA-PHBV-PLA. The latter were all electrospun and then all four scaffolds (three synthetic, one natural) were placed in six well plates. A culture well was formed on the scaffold using a 1 cm diameter stainless steel ring and 1.5×10^5 oral fibroblasts were seeded one side; after two days of culture, the ring was placed on the other side of the scaffolds and 3×10^5 oral keratinocytes were seeded on to the scaffolds and cultured with keratinocytes uppermost. After a further two days of culture, scaffolds were cut to 1 cm² and raised to an air-liquid interface on stainless steel grids; some were treated with 200 μ g/mL β -APN throughout the culture period (28 days). Contraction in vitro was assessed by serial digital photography of cell-seeded scaffolds and cell-free scaffolds three times a week for 28 days. All cell-seeded scaffolds were assessed for cell metabolic activity, mechanical properties, histology, and morphology by scanning electron microscopy (SEM).

Results: The mean fibre diameters and pore sizes of PLA and PHBV scaffolds were 2.4 ± 0.77 , 0.85 ± 0.21 μ m ($p < 0.001$), and 10.8 ± 2.3 , 4.3 ± 1.1 μ m ($p < 0.001$), respectively. Oral fibroblasts and keratinocytes were tightly adhered and grew well on both surfaces of trilayer. The ultimate tensile strength (UTS) and Young's modulus (YM) of PLA samples were significantly lower than Euroskin ($p < 0.001$ and $p < 0.05$, respectively); only the UTS of the trilayer samples was slightly significantly lower ($p < 0.05$). Metabolic activity was significantly increased for cells on all scaffolds, without significant differences between them from Day 0 to Day 28. There were no

adverse effects of β -APN on cell viability. With respect to contraction, cells on trilayer and PHBV monolayers did not undergo any significant contraction; however, cells on PLA monolayer and Euroskin contracted 25.3% and 56.4%, respectively, over 28 days. The addition of 200 μ g/mL β -APN significantly reduced contraction of Euroskin compared with the control ($p < 0.01$); however, β -APN did not affect PLA contraction during this culture period ($p > 0.05$).

Conclusions: This study shows that a trilayer micro-nano-3D porous synthetic scaffold is suitable for oral keratinocyte and fibroblast growth with good cell viability and minimal contraction. This material also has good mechanical properties and histological analyses showed its ability to mimic normal human oral mucosal morphology. Furthermore, synthetic trilayer scaffolds have advantages over biological scaffolds — there is no risk of disease transmission or immunological rejection and they appear resistant to contraction. We suggest they present a good alternative to allodermis for future use in urethral reconstruction.

Introduction

Urethral strictures are an abnormal narrowing of the urethra that can be due to iatrogenic, idiopathic, inflammatory, or traumatic causes. The most common etiology of urethral stricture is idiopathic (41%), followed by iatrogenic (35%).

Iatrogenic injuries are related to placing of indwelling catheters, transurethral manipulation, surgery for hypospadias, prostatectomy, and brachytherapy.^{1,2} Overall, the incidence of urethral strictures is about 1% for males over the age of 55 years. The actual incidence differs based on worldwide populations, geography, and income.^{3,4}

Treatment of urethral strictures depends on stricture etiology, localization, stricture length, the degree of spongiosclerosis, the previous history of treatment, and the patient's age. Short, simple strictures are treated endoscopically; however, longer, more complex strictures in the penile urethra often require a one- or two-stage urethroplasty. In carrying out an augmentation procedure, a range of materials have been used for grafting, including penile skin, scrotal skin, oral mucosa, bladder mucosa, and colonic mucosa. From these,

oral mucosa grafts have become the most clinically effective due to their short harvest time, lack of hair, low associated morbidity, and high clinical success rates.⁵⁻⁸

Reported complications of oral mucosal grafts include intraoperative hemorrhage, postoperative infection, pain, swelling, and damage to salivary ducts.^{9,10} In particular, it can be difficult to obtain enough buccal mucosa for long grafts. Accordingly, to reduce donor site morbidity, tissue-engineered buccal grafts have been used as an alternative for reconstruction of complex urethral strictures.

In 2004, our group developed tissue-engineered buccal mucosa (TEBM) based on allogeneic cadaveric dermal tissue and autologous cultured buccal mucosa keratinocytes and fibroblasts for reconstruction of the urethra.¹¹ In 2008, we reported the three-year outcomes of a first clinical trial of this material in five patients.^{11,12} We found that initial results were good in all five patients, with rapid vascularisation of the grafts allowing successful retubularisation of all patients as though native buccal mucosa had been used. However after eight and nine months, respectively, two of the five patients' grafts developed contraction and fibrosis; this affected part of the graft for one patient and all of the graft for another. Our nine-year followup of these patients published in 2014 showed no further fibrosis for the four patients who still had TEBM buccal mucosa in place.¹³

We have more recently looked beyond using native dermis as a scaffold for TEBM for two reasons: eliminating any risk of infection and reducing graft contracture. With donor grafts, there is always a potential, albeit small risk, of disease transmission. This can be mitigated by accessing cadaveric skin from accredited tissue banks where donors are screened for bacteria and Hepatitis B and C, and efforts are made to exclude patients carrying HIV (the latter is the most challenging, as there is a period of seroconversion in which a patient may be infected and yet not test positive). Clearly, with cadaveric donation, this will always remain a small risk.

The other reason that we have moved to synthetic dermal substrates is to see if we can overcome some of the problems of graft contraction and fibrosis. Therefore, we developed synthetic electrospun biodegradable scaffolds for urethral reconstruction.¹⁴ We have also explored using drug approaches to prevent contraction of dermal-based scaffolds used in tissue engineered skin production.¹⁵

In this study, we have explored the production of TEBM using de-epidermised acellular dermis, in this case sourced from an accredited tissue bank (Euroskin) and compared it to buccal mucosa based on three synthetic scaffolds: Poly-L-lactic acid (PLA), Poly(3-hydroxybutyrate-co-3-hydroxyvalerate) (PHBV), and a trilayer scaffold, which consists of microfibers of PLA and nanofibers of PHBV.

PLA has a long history of use and is well-known to be a biodegradable biomaterial with good biocompatibility.^{16,17} It has been used extensively in our group¹⁸⁻²¹ for applications

ranging from a material for repair of the pelvic floor²¹ to a combination of PLA with polyglycolic acid (PGA), as PLGA, to make a biodegradable scaffold for use in the cornea.²² The second polymer, PHVB, was selected because it can be readily spun into nanofibrous layers,²³ and when combined with microfibers of PLA, can produce a microporous/nanoporous/microporous trilayer that mimics, to some extent, the architecture of skin in that the PHBV fibres can be produced as a thin compact layer acting as a pseudo-basement membrane. This allows the segregation of different cell types.^{23,24}

The aim of this study was to improve on the development of TEBM for future clinical use by comparing a synthetic trilayer (PLA-PHBV-PLA) biodegradable alternative to human dermis, and further, to explore the use of beta-aminopropionitrile (β -APN) as a lysyl oxidase inhibitor to reduce contraction in these grafts.

Methods

Preparation of PLA and PHBV monolayer scaffolds

PLA (Goodfellow, Cambridge, U.K.) was dissolved in dichloromethane (DCM) at 10% wt PLA. PHBV (Goodfellow, Huntingdon, U.K.) was dissolved in 90 wt% DCM/10 wt% methanol solution. For random scaffolds, polymer solutions were loaded into 5 mL syringes fitted with blunt tipped stainless steel needles with an internal diameter of 0.8 mm (I&J Fisnar Inc.). Four syringes with 5 mL solution in each were used to deliver the solutions at a constant flow rate of 2.4 mL/h using a programmable syringe pump (Genic, Kent Scientific, U.S.). Solutions were electrospun horizontally with an accelerating voltage of 17 kV supplied by a high-voltage power supply (Model 73030 P, Genvolt, Shropshire, U.K.). Fibrous mats were collected on aluminium foil sheets (18×16 cm) wrapped around an earthed aluminium rotating collector (rotating at 300 r/min) 17 cm (PLA), 10 cm (PHBV) from the tip of the needle.

Preparation of PLA-PHBV-PLA trilayer scaffold

Micro-fibrous PLA and nano-fibrous PHBV trilayer scaffolds were electrospun using parameters as described by Bye et al.²⁴ PLA and PHBV solution were pumped from four syringes at 2.4 mL/h per syringe. For PLA, a needle to collector distance of 17 cm was used, while for PHBV, a distance of 10 cm was used. The syringe needles were charged to +17 kV and polymer solutions spun onto an earthed rotating (300 RPM) aluminium foil coated mandrel. PLA and PHBV were setup in separate syringe pumps on either side of the rotating mandrel and charged by individual power supplies. Trilayers were spun by sequentially spinning first 8 ml PLA, then 4 ml of PHBV simultaneously with 4 ml PLA from a matching

spinning setup on the other side of the mandrel, then 8 ml PLA alone, creating a PLA-PHBV-PLA trilayer construct.

Preparation of DED from Euroskin

We have previously shown that tissue-engineered skin can be prepared from either cadaveric skin treated in-house or from the Dutch Tissue Bank, Euroskin purchased commercially.²² Accordingly, in this study, we used Euroskin as our source of cadaveric dermis. Euroskin was purchased from Euroskin Bank, Netherlands, after seeking approval to use this material for research purposes.

The glycerol preserved EuroSkin was washed several times with phosphate-buffered saline (PBS) until the glycerol was washed away. This was then de-epidermised by immersion in 1-M sodium chloride for 24 hours, and the epidermis was removed with gentle scraping with forceps. Euroskin was then washed thoroughly with PBS and placed in medium at 37 °C for 2–3 days to confirm sterility. It was then incubated rehydrated in antibiotic-free media for 48 hours prior to use.

Isolation and culture of oral keratinocytes and fibroblasts

Oral biopsies comprising of 0.5 cm² of tissue were taken after informed consent and ethical approval from healthy volunteers or patients undergoing buccal mucosa removal for urethroplasty or for dental procedures (003463/2015). Specimens were washed with PBS containing 100 mg/mL streptomycin and 100 IU/mL penicillin. The tissue samples were then incubated overnight (12–18 hours) at 4 °C in 0.1% w/v trypsin solution. Epidermal and dermal layers were peeled apart, and keratinocytes were isolated from the lower surface of the epidermis and the upper surface of the dermis by gentle scraping with a scalpel blade. Keratinocytes were then seeded at a density of 2x10⁶ per T75 culture flask pre-seeded for 24 hours with 5x10⁵ i3T3 cells in Green's keratinocyte medium; DMEM and Ham's F12 medium in a 3:1 ratio supplemented with 10% FCS, 10 ng/mL EGF, 0.4 µg/mL hydrocortisone, 10⁻¹⁰ mol/mL cholera toxin, 1.8x10⁻⁴ mol/L adenine, 5 µg/mL insulin, 2x10⁻³ mol/L glutamine, 2x10⁻⁷ mol/L triiodothyronine, 0.625 µg/mL amphotericin B, 100 IU/mL penicillin, and 100 µg/mL streptomycin.²⁵ Keratinocytes were maintained in culture to passage three, then used in experiments. Fibroblasts were isolated from the dermis remaining after keratinocyte isolation. The dermis was washed with PBS then finely minced and placed in 10 mL of 0.5% w/v collagenase A at 37 °C in a humidified CO₂ incubator for 18–20 hours. After centrifugation of the resulting cell suspension at 400 g for 10 minutes, cells were then cultured in DMEM media supplemented with 10% FCS 2x10⁻³ mol/L glutamine, 1.25 µg/mL amphotericin B, 100 IU/mL penicillin, and 100 µg/mL streptomycin. Fibroblasts were used in experiments between passages four and nine.

Cell seeding on scaffolds

Trilayer (PLA-PHBV-PLA) and monolayer (PLA, PHBV) electrospun scaffolds (2x2 cm) were sterilized (using 70% v/v ethanol in dH₂O) for 10 minutes, washed with PBS, and placed in six well plates. A 1 cm diameter culture well was formed on the scaffold using a 1 cm diameter stainless steel ring and 1.5x10⁵ oral fibroblasts seeded inside. Constructs were cultured for two days at 37 °C and 5% CO₂. Scaffolds were then turned over and 3x10⁵ oral keratinocytes were seeded onto each scaffold in Green's medium. After a further two days of culture, scaffolds were cut to 1 cm² and raised to an air-liquid interface (this was counted as Day 1) on stainless steel grids; some were treated with 200 µg/mL β-APN throughout the culture period of 28 days. Samples were run in triplicate and experiments were repeated three times for contraction and cell viability (n=9).

Cell seeding on dermis prepared from Euroskin

Dermis prepared from Euroskin was cut into 2x2 cm² pieces and each placed in a six-well plate. Oral fibroblasts were seeded on the inside of a 1 cm diameter stainless steel ring at 1.5x10⁵ after two days cultured; Euroskin was turned over and 3.0x10⁵ oral keratinocytes were seeded. Grafts were cultured for 48 hours submerged and then cut to 1 cm² diameter and raised to air-liquid interface for the remainder of the assessment period. Samples were run in triplicate and experiments were repeated three times for contraction and cell viability (n=9).

Measurement of contraction of scaffolds

Contraction in vitro was assessed by serial digital photography cell-seeded scaffolds and cell-free scaffolds for three times a week until the end of the experiment. Images were analysed using ImageJ software (National Institutes of Health, Bethesda, MD, U.S.).

Assessment of cell viability

Cell metabolic activity was measured by a resazurin assay. Before air-liquid interface, samples were washed with PBS and 5 mL of 50 µg/mL resazurin in PBS was added. Samples were incubated for 60 minutes at 37 °C. Then absorbance at 570 nm was measured in a colourimetric plate reader (Bio-TEK, NorthStar Scientific Ltd, Leeds, U.K.). Samples were then washed with PBS and returned to culture conditions. Cell viability testing was repeated after three, seven, 14, 21, and 28 days of culture.

Mechanical testing of scaffolds

A total of six samples each (n=6), trilayer (PLA-PHBV-PLA), PLA, PHBV, and Euroskin were cut and the width and thickness were measured using a ruler and micrometer, respectively. These scaffolds were then clamped on a tensiometer (BOSE Electroforce Test Instruments). A load of 22 N and a ramp test at a rate of 0.1 mm/s was applied. The strain was normalized to the length of the samples. The stress was normalized by the area (width x thickness). The first failure point or plateau was used to calculate the ultimate tensile strength (UTS) and the displacement at this point for the ultimate tensile strain (UT strain). The Young's Modulus (YM) was then calculated.

Scanning electron microscopy (SEM) of scaffolds

The morphology of prepared PLA, PHBV, and trilayer (PLA-PHBV-PLA) scaffolds were observed through SEM (gold sputtering- Emscope SC 500A Sputter Coater), which was imaged with a FEI Inspect F scanning electron microscope (Cambridge, U.K.).

Fibre diameters and pore sizes were quantified from SEM images of electrospun scaffolds. From each sample (n=6), four images were selected and 10 fibres and five pores per image analyzed for fibre diameter and pore size, respectively. This gave a total of 240 fibres and 120 pores analyzed per scaffold. The software ImageJ (National Institutes of Health) was used for quantification. Pores were identified as areas of void space bounded by fibres on all sides at or near the same depth of field.

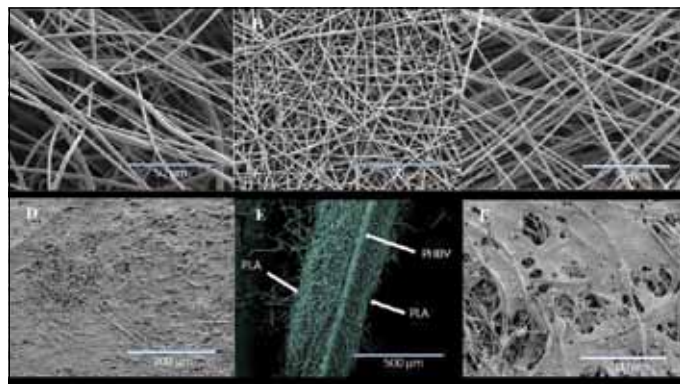


Fig. 1A. Scanning electron micrograph (SEM) of electrospun scaffolds (A) poly-L-lactic acid (PLA); (B) poly(3-hydroxybutyrate-co-3-hydroxyvalerate)(PHBV); and (C) trilayer (PLA-PHBV-PLA). (D) Oral fibroblast cells are tightly adhered on the lower surface of the trilayer and growing well. (E) Cross-section of trilayer. (F) Oral keratinocytes are grown and stretched well on the upper layer of the trilayer scaffolds.

Histological evaluation of scaffolds

Scaffolds were embedded with OCT compound and frozen in liquid nitrogen. Scaffold cross-sections (5 or 10 μ m thickness) were cut with a cryostat (Leica CM300) and placed on frosted slides. The sample-carrying slides were then soaked in deionised water (two minutes) to remove the OCT, stained with hematoxylin (1.5 minutes), washed with running tap water (four minutes), and stained with eosin (five minutes). After another wash with tap water (five minutes), samples were dehydrated in 70% alcohol, followed with the immersion in 100% alcohol. Finally, the slides were cleaned twice in xylene and mounted with a coverslip by using a DPX mounting medium. Slides were observed by a light microscope.

Statistics

The results were presented as the mean \pm standard deviation (SD). Data were analysed with independent sample T-test and analysis of variance (ANOVA) to determine the difference among groups using SPSS 23 software program. Differences in mechanical properties were statistically tested with a GraphPad Prism 8 software using a Friedman test and doing multiple comparisons between individual groups using a Dunn's test. A p value < 0.05 was considered statistically significant.

Results

Characterization of scaffolds and cells cultured on scaffolds

SEM and histological images of the scaffolds are shown in Figs. 1A and 1B. The mean fibre diameters and pore sizes

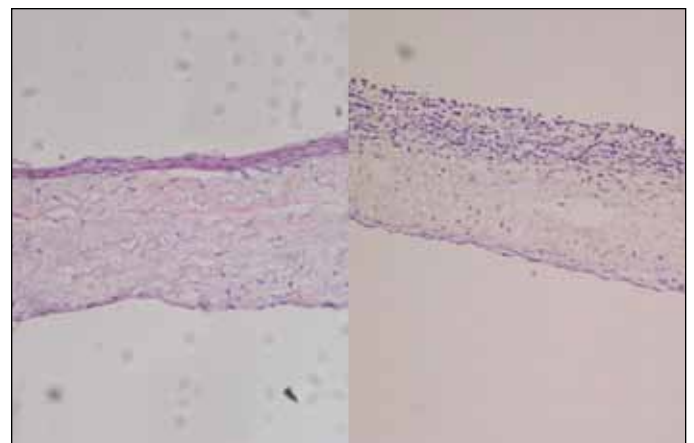


Fig. 1B. Histological appearance of tissue-engineered buccal mucosa using (A) Euroskin; and (B) trilayer (PLA-PHBV-PLA). Oral keratinocytes were seeded on the upper surface and fibroblasts were seeded on the lower surface of the scaffolds and stained with haematoxylin and eosin after culture periods (magnification X10)

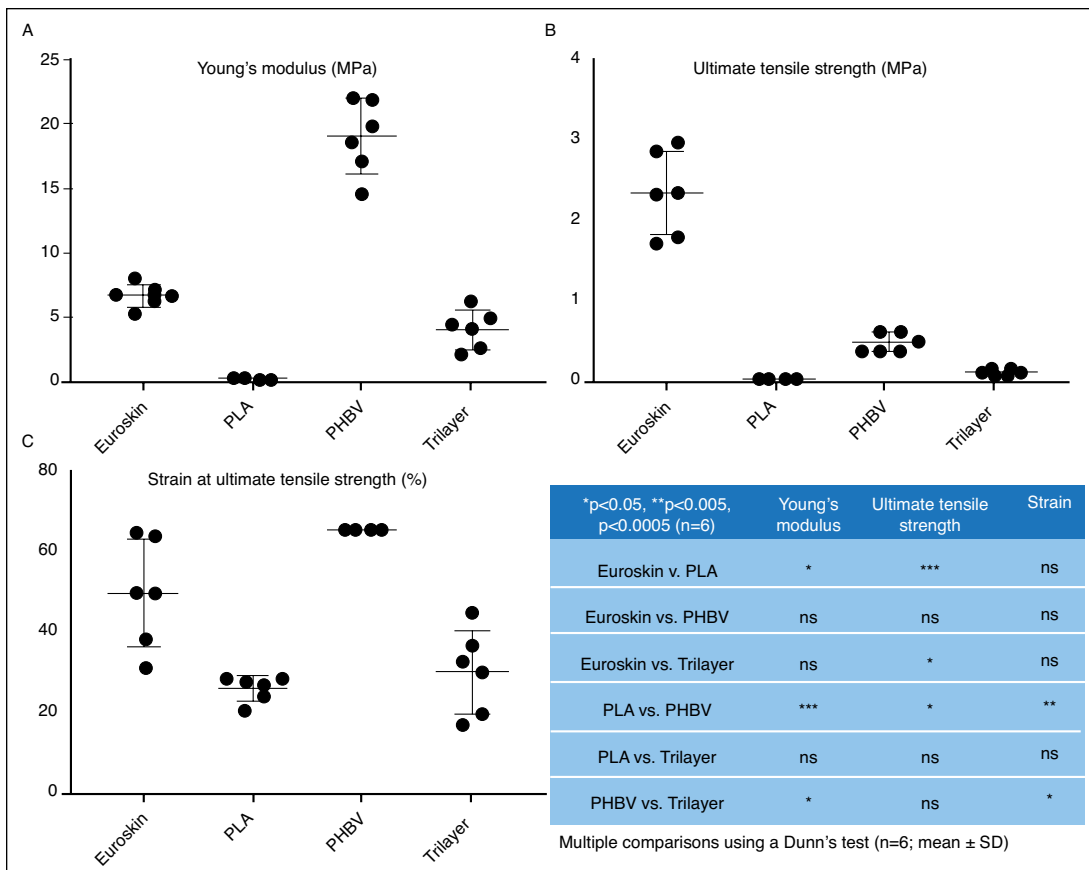


Fig. 2. Mechanical properties mean ± standard deviation (SD) values for Young's modulus and tensile strength and strain at ultimate tensile strength. ns: not significant; PLA: poly-L-lactic acid; PHBV: poly(3-hydroxybutyrate-co-3-hydroxyvalerate); SD: standard deviation.

of PLA and PHBV scaffolds were 2.4 ± 0.77 and 0.85 ± 0.21 μm for fibre diameter, respectively ($p < 0.001$), and 10.8 ± 2.3 and 4.3 ± 1.1 μm for pore size, respectively ($p < 0.001$). Porosity measurements showed a significant difference between the microfibrinous scaffolds (as shown in Fig. 1A (A)) and the nanofibrinous scaffolds (shown in Fig. 1A (B)), with the microfibrinous PLA being around 28% more porous. Fig. 1A (E) shows a cross-section through this trilayer scaffold in which it can be seen that the overall thickness of the scaffold was around 400 μm , while the thickness of the PHBV layer was around 30 μm .

Fig. 1A also shows culture of oral fibroblasts on the lower surface of the trilayer scaffold (D) and of oral keratinocytes on the upper surface of the trilayer scaffold (F). Fig. 1B shows H&E histology of oral keratinocytes and fibroblasts cultured on TEBM made based on Euroskin (A) vs. TEBM made using the trilayer of PLA/PHBV/PLA (B). This shows a decent number of fibroblasts in the lower layer and a much thicker layer of keratinocytes on the upper surface for both.

Mechanical properties of the scaffolds

Fig. 2 compares the YM, UTS, and UT strain of Euroskin and three synthetic scaffolds. There are significant differ-

ences between the groups shown by one-way ANOVA ($p < 0.001$) and the tables in Fig. 2 show multiple statistical comparisons between these.

Compared to Euroskin, UT strain was not significantly different for any of the three synthetic scaffolds. However, the UTS and YM of PLA samples were significantly lower than that of Euroskin ($p < 0.001$ and $p < 0.05$, respectively). While these two properties were not significantly different for PHBV samples compared to Euroskin, only the UTS of the trilayer samples was significantly lower ($p < 0.05$).

Cell viability on scaffolds

Fig. 3 shows cell viability of the cells on the scaffolds assessed throughout 28 days of culture using a resazurin salt assay. Metabolic activity was significantly increased for all groups over time without there being any significant differences between cells grown on the different scaffolds. Additionally, there was no effect of the addition of 200 μm β -APN on cell viability for cells growing on these scaffolds.

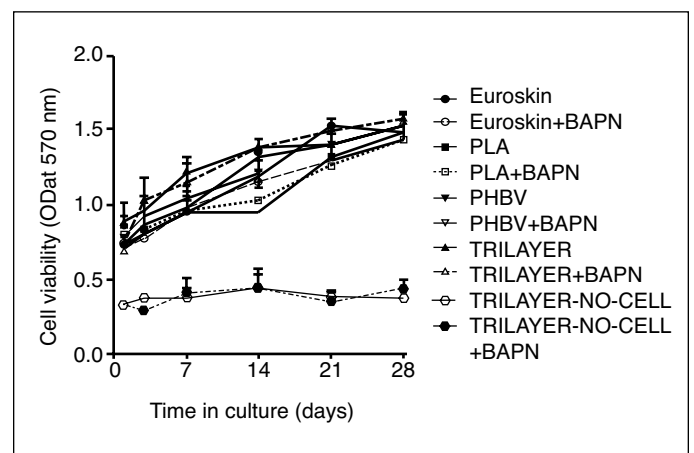


Fig. 3. Cell viability of oral keratinocytes and fibroblasts grown on scaffolds. β -APN: beta-amino-propionitrile; PLA: poly-L-lactic acid; PHBV: poly(3-hydroxybutyrate-co-3-hydroxyvalerate).

The figure also shows that there was no evidence any metabolic activity for Euroskin cultured on its own.

Contraction of scaffolds by keratinocytes and fibroblasts

Fig. 4 shows the appearance of these buccal mucosa constructs at Days 1 and 28 when based on Euroskin, showing extensive contraction slightly reduced by the addition of β -APN. In contrast, cells on the trilayer show little contraction by Day 28 and the addition of β -APN was without effect.

Fig. 5 shows the extent to which the cells on different scaffolds contracted the scaffold and the effect of 200 μ m β -APN on this. It was very evident that, as previously reported, the keratinocytes and fibroblasts contracted the tissue-engineered constructs when these were based on natural dermis from Euroskin. The addition of β -APN significantly reduced contraction of these scaffolds ($p < 0.01$).

For the other three scaffolds, PLA, PHBV and the trilayer, the extent of contraction over 28 days was much less and was not significantly affected by the addition of 200 μ g/ml β -APN. These results are summarized in Table 1.

Discussion

The need for tissue-engineered grafts was identified for those patients who require treatment for recurrent, long, complex urethral strictures.²⁶ In the initial treatment of long, complex urethral strictures, autologous buccal mucosa was



Fig. 4. Appearance of tissue engineered scaffolds at (A, E) Day 1; (B, F) Day 28 based on Euroskin and trilayer and the absence (A, B, E, F) and presence (C, D, G, H) of β -APN. β -APN: beta-amino-propionitrile.

shown to be successful. However, the urethral re-stricture rate remains significant at 14.5–15.7%.²⁷ Treatment of recurrent strictures can be more difficult because of urethral shortening from prior surgery, the degree of inflammation of the urethra, and the spongioblastic fibrosis and periurethral scarring itself and associated poor blood supply. For these challenging patients, it may be possible to harvest further autologous buccal tissue, but with increasing likelihood of donor site complications. In some cases, because of prior surgery, this may not be possible. Accordingly in recent years, TEBM has been explored for urethral reconstruction.

Our previous studies looking at tissue-engineered skin have identified that it is the epithelial cells rather than the

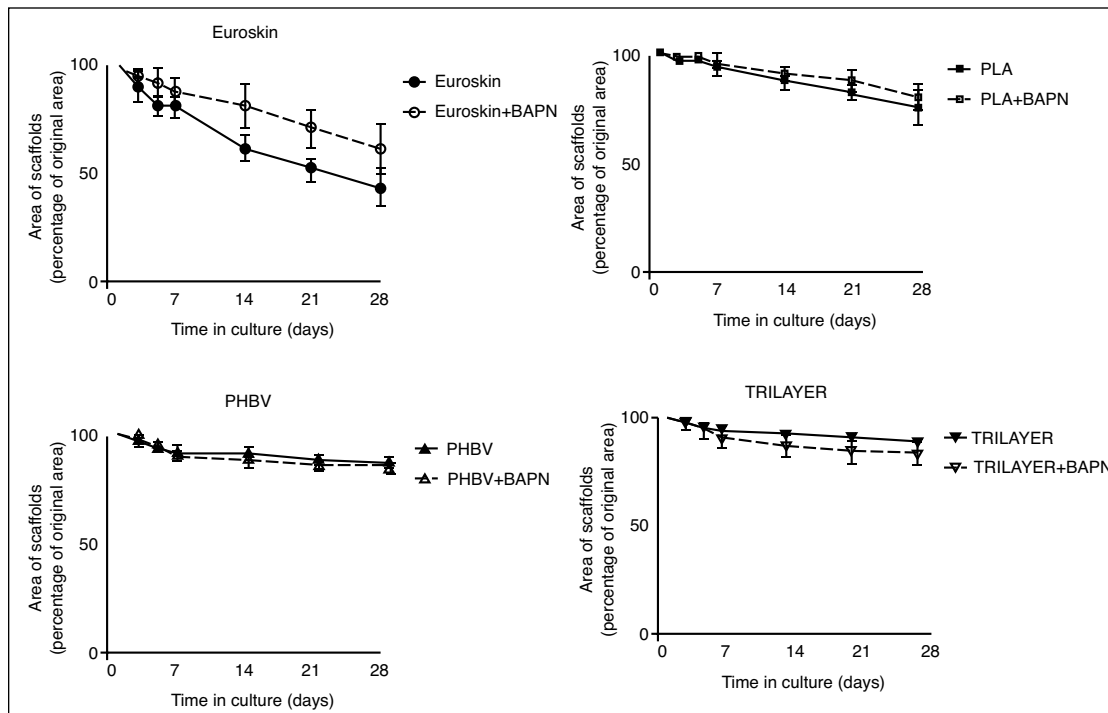


Fig. 5. Time course of scaffold contraction. β -APN: beta-amino-propionitrile; PLA: poly-L-lactic acid; PHBV: poly(3-hydroxybutyrate-co-3-hydroxyvalerate).

Table 1. Contraction of scaffolds by oral keratinocytes and fibroblasts over 28 days in the presence and absence of β -APN

Group	Day 1	Day 3	Day 5	Day 7	Day 14	Day 21	Day 28
Euroskin	100	89.4 \pm 6.9	81.1 \pm 4.6	82.2 \pm 6.0	61.4 \pm 6.1	51.6 \pm 5.7	43.6 \pm 9.1
Euroskin + β -APN	100	94.1 \pm 4.1	91.3 \pm 8.0	87.1 \pm 7.4	80.3 \pm 11.9	70.8 \pm 8.1	61.1 \pm 11.6
PLA	100	97.2 \pm 2.3	96.7 \pm 0.9	93.7 \pm 1.2	87.3 \pm 4.3	82.4 \pm 5.0	74.7 \pm 8.4
PLA+ β -APN	100	99.8 \pm 3.1	97.8 \pm 2.5	94.2 \pm 5.1	90.3 \pm 3.3	86.9 \pm 6.1	80.1 \pm 6.1
PHBV	100	95.2 \pm 1.5	91.9 \pm 1.6	91.3 \pm 2.9	89.9 \pm 3.1	87.8 \pm 2.1	86.3 \pm 2.1
PHBV+ β -APN	100	98.3 \pm 1.2	94.1 \pm 2.3	90.2 \pm 3.8	88.2 \pm 3.9	85.4 \pm 3.1	84.8 \pm 8.1
TRILAYER	100	97.4 \pm 1.8	95.6 \pm 0.5	95.2 \pm 2.2	93.7 \pm 1.0	90.8 \pm 2.2	88.1 \pm 2.4
TRILAYER+ β -APN	100	97.1 \pm 2.3	94.7 \pm 3.6	91.1 \pm 5.6	87.0 \pm 5.5	86.8 \pm 6.0	86.5 \pm 7.5

Values are mean \pm standard deviation (SD). The contractions of the scaffolds were calculated by dividing the area of each scaffold at the termination of the culture period by its original area (first day area). (Area*100/original area). β -APN: beta-amino-propionitrile; PLA: poly-L-lactic acid; PHBV: poly(3-hydroxybutyrate-co-3-hydroxyvalerate).

stromal fibroblasts that drive the contraction by stimulating the enzyme lysyl oxidase that crosslinks collagen fibres.²⁸ A pharmacological study revealed that an inhibitor of lysyl oxidase, β -APN (found in the sweet-pea family), was capable of significantly reducing contraction. We have also previously explored a few other routes to block or resist contraction. The most promising of these was to suture the graft in place against a rigid framework in the laboratory for the first seven days, and this seems to reduce the extent of the contraction.²⁹

The aim of this study was to explore alternative synthetic scaffolds as substrates for the production of TEBM for future use in reconstruction of the urethra. As part of this, we explored the addition of an inhibitor of the collagen crosslinking enzyme lysyl oxidase, β -APN, to see to what extent this might reduce the cell-induced contraction of these grafts in vitro.

The main findings of this study were that it is possible to make a trilayer scaffold out of microfibers of PLA and nanofibers of PHBV, which supported the production of a TEBM. The mechanical properties of the trilayer were comparable to those of TEBM based on native dermis, but encouragingly, cells showed relatively little ability to contract these in vitro. We found β -APN reduced the contraction of the construct when cells were cultured on native dermal collagen, but had no effect on the very slight degree of contraction seen when the cells were cultured on the trilayer scaffold.

In this study, we designed a scaffold based on a combination of PLA and PHBV. PLA is a FDA-approved, synthetic, biodegradable, biocompatible polymer of lactic acid produced by ring opening polymerisation of lactic acid. It is a hydrophobic, semi-crystalline, and amorphous polymer.³⁰ It has been used as a biomaterial for a variety of different urological applications.^{18,19,31,32} In our comparisons, we studied electrospun PLA on its own and showed that it is a good substrate for the growth of oral keratinocytes and fibroblasts. However, it has relatively poor mechanical properties compared to Euroskin. Cells grown on PLA scaffolds showed approximately 25% contraction.

The second polymer, PHBV, is a natural, biodegradable polymer formed by bacterial fermentation; it has been electrospun into fibrous scaffolds for a wide range of applications,^{33,34} including skin grafts, drug-delivery systems, cartilage tissue engineering, and reconstructive implants.³⁵⁻³⁸ It is relatively hydrophobic, with a longer and much slower rate of degradation, which can be seen as disadvantages.³⁹ It is often used in combination with other polymers to obtain new materials.⁴⁰

We developed a trilayer scaffold in which PHBV was used to produce a pseudo-basement membrane of nanofibers, separating oral keratinocytes from oral fibroblasts. We previously demonstrated that a nanofibrous scaffold can act as a barrier for cell penetration,²³ while a microfibrillar scaffold provides cell attachment and proliferation for two different cell types.

With respect to the UTS, the trilayer was 0.13 \pm 0.035 compared to 2.34 \pm 0.67 for Euroskin. We suggest it is not essential that the mechanical properties are exactly as for the native tissue, but that they are "good enough" to maintain a patent urethra long-term.

The trilayer scaffolds presented the closest values for stiffness and stretchability compared to that of Euroskin. The addition of the nanofibrous component of the trilayer made a material with mechanical properties closer to native tissues, and it was easy to handle. By this we mean that it could be picked up, shaped, and handled without tangling, sticking, or losing its shape.

In a previous study, we tried to use oral mucosal cells seeded on a synthetic biodegradable scaffold made of polylactic-co-glycolic acid (PLGA) for urethral reconstruction.¹⁴ However, all scaffolds showed extensive contraction (more than 50% over 14 days) irrespective of the method of sterilization or the presence of cells. This was unsatisfactory.

Wei et al prepared a polycaprolactone/silk/collagen nano-3D porous scaffold for urethral reconstruction. They showed that oral mucosal epithelial cells grew well on the scaffold. However, these authors did not comment on scaffold contraction and evaluated cell viability for only seven days.⁴¹ Another study evaluated the capacity of a PLA scaffold seeded with rabbit adipose tissue-derived stem cells to

repair a urethral defect in a rabbit model. After four or six weeks of implantation, the grafts were collected and analyzed histologically. Their data demonstrated good integration into native tissues and they concluded that cell-seeded PLA-based materials would be good candidates for the next generation of tissue-engineered urethras.⁴²

Raya-Rivera et al reported the outcomes of five male patients who underwent urethroplasty. They took bladder tissue biopsy from each patient and cells were expanded and seeded onto tubularized PLGA scaffolds; 4–6 cm manufactured scaffolds were used for urethral reconstruction. After 71 months, median followup serial radiographical, urinary flow rate, and endoscopic studies showed the maintenance of wide urethral calibres without strictures. The authors concluded that tubularized urethra can be engineered to be used as a prospective clinical procedure.⁴³ However, this was just a small clinical trial that required an invasive bladder biopsy using a suprapubic incision, which carries risks of serious complications.⁴³

Our group has experience on contraction of tissue-engineered skin and we have previously demonstrated that extensive collagen crosslinking is related to contraction.²⁸ This can be reduced by the inhibition of lysyl oxidase, a key enzyme involved in collagen crosslinking.²⁹ The current study showed that β -APN significantly inhibited Euroskin contraction, however, this effect was not seen in PLA scaffolds. This may be explained by the lower collagen levels found in the PLA scaffolds compared to the natural dermal substrates.

In this study, we successfully seeded oral keratinocytes and fibroblasts on each side, respectively, of PLA-PHBV-PLA micro-nano-3D porous scaffolds. Cells grew well on both PLLA sides of the membrane and the PHBV barrier membrane provided a barrier against cell infiltration between the different cells on the PLLA scaffolds on either side of the barrier.

A limitation of this study is that while it is ideal for looking at short-term contraction over several weeks in vitro, it cannot shed light on the complex issue of fibrosis, which can occur many months post-implantation. In our study, it occurred in two patients eight and nine months post-implantation, strongly suggesting that this is an immune system-triggered process.¹² These patients suffered from recurrent fibrosis throughout the previous 10 years before transplantation of TEBM. The other patients maintained luminal patency throughout the following nine years of followup.¹³

It might, in the future, be possible to deliver a lysyl oxidase inhibitor as part of a drug-eluting scaffold, but we have to point out that there are very few studies as yet looking at the process of fibrosis post-implantation of TEBM. The fact that this can occur many months post-implantation suggests that this will be a challenge to study and it may not be a process that can be studied in animal models if the trigger is an underlying recurrent inflammatory process.

Conclusion

A PLA-PHBV-PLA trilayer micro-nano-3D porous scaffold is suitable for oral keratinocyte and fibroblast growth, with good cell viability and minimal contraction. This cell-loaded material also has good mechanical properties and histological analyses showed its ability to mimic normal human oral mucosal morphology for tissue-engineered urethral reconstruction. Furthermore, trilayer scaffolds have the advantage over biological scaffolds for avoiding immunological rejection and preventing viral infections. Further investigations are necessary to translate this in vitro technology into preclinical and clinical studies.

Competing interests: The authors report no competing personal or financial interests related to this work.

Funding: Dr. Simsek was funded by the Scientific and Technological Research Council of Turkey.

This paper has been peer-reviewed.

References

- Lumen N, Hoebeke P, Willemsen P, et al. Etiology of urethral stricture disease in the 21st century. *J Urol* 2009;182:983-7. <https://doi.org/10.1016/j.juro.2009.05.023>
- Fenton AS, Morey AF, Aviles R, et al. Anterior urethral strictures: Etiology and characteristics. *Urology* 2005;65:1055-8. <https://doi.org/10.1016/j.urol.2004.12.018>
- Anger JT, Buckley JC, Santucci RA, et al. Trends in stricture management among male Medicare beneficiaries: Underuse of urethroplasty? *Urology* 2011;77:481-5. <https://doi.org/10.1016/j.urol.2010.05.055>
- Santucci RA, Joyce GF, Wise M. Male urethral stricture disease. *J Urol* 2007;177:1667-74. <https://doi.org/10.1016/j.juro.2007.01.041>
- Lumen N, Oosterlinck W, Hoebeke P. Urethral reconstruction using buccal mucosa or penile skin grafts: Systematic review and meta-analysis. *Urologia Int* 2012;89:387-94. <https://doi.org/10.1159/000341138>
- Barbagli G, Sansalone S, Djinic R, et al. Current controversies in reconstructive surgery of the anterior urethra: A clinical overview. *Int Braz J Urol* 2012;38:307-16.
- Barbagli G. When and how to use buccal mucosa grafts in penile and bulbar urethroplasty. *Italian J Urology Nephrol* 2004;56:189-203.
- Markiewicz MR, Lukose MA, Margaroni JE, et al. The oral mucosa graft: A systematic review. *J Urol* 2007;178:387-94. <https://doi.org/10.1016/j.juro.2007.03.094>
- Jang TL, Erickson B, Medendorp A, et al. Comparison of donor site intraoral morbidity after mucosal graft harvesting for urethral reconstruction. *Urology* 2005;66:716-20. <https://doi.org/10.1016/j.urol.2005.04.045>
- Das SK, Kumar A, Sharma GK, et al. Lingual mucosal graft urethroplasty for anterior urethral strictures. *Urology* 2009;73:105-8. <https://doi.org/10.1016/j.urol.2008.06.041>
- Bhargava S, Choppe CR, Bullock AJ, et al. Tissue-engineered buccal mucosa for substitution urethroplasty. *BJU Int* 2004;93:807-11. <https://doi.org/10.1111/j.1464-410X.2003.04723.x>
- Bhargava S, Patterson JM, Inman RD, et al. Tissue-engineered buccal mucosa urethroplasty-clinical outcomes. *Eur Urol* 2008;53:1263-9. <https://doi.org/10.1016/j.eururo.2008.01.061>
- Osman NI, Patterson JM, MacNeil S, et al. Long-term followup after tissue-engineered buccal mucosa urethroplasty. *Eur Urol* 2014;66:790-1. <https://doi.org/10.1016/j.eururo.2014.07.007>
- Selim M, Bullock AJ, Blackwood KA, et al. Developing biodegradable scaffolds for tissue engineering of the urethra. *BJU Int* 2011;107:296-302. <https://doi.org/10.1111/j.1464-410X.2010.09310.x>
- Harrison CA, Heaton MJ, Layton CM, et al. Use of an in vitro model of tissue-engineered human skin to study keratinocyte attachment and migration in the process of reepithelialization. *Wound Rep Regen* 2006;14:203-9. <https://doi.org/10.1111/j.1743-6109.2006.00111.x>

16. Engelhardt EM, Micol LA, Houis S, et al. A collagen-poly (lactic acid-co-varepsilon-caprolactone) hybrid scaffold for bladder tissue regeneration. *Biomaterials* 2011;32:3969-76. <https://doi.org/10.1016/j.biomaterials.2011.02.012>
17. Telemeco TA, Ayres C, Bowlin GL, et al. Regulation of cellular infiltration into tissue engineering scaffolds composed of submicron diameter fibrils produced by electrospinning. *Acta Biomaterialia* 2005;1:377-85. <https://doi.org/10.1016/j.actbio.2005.04.006>
18. Roman S, Mangir N, Bissoli J, et al. Biodegradable scaffolds designed to mimic fascia-like properties for the treatment of pelvic organ prolapse and stress urinary incontinence. *J Biomater Appl* 2016;30:1578-88. <https://doi.org/10.1177/0885328216633373>
19. Mangir N, Bullock AJ, Roman S, et al. Production of ascorbic acid releasing biomaterials for pelvic floor repair. *Acta Biomaterialia* 2016;29:188-97. <https://doi.org/10.1016/j.actbio.2015.10.019>
20. Sharma K, Bullock A, Ralston D, et al. Development of a one-step approach for the reconstruction of full thickness skin defects using minced split thickness skin grafts and biodegradable synthetic scaffolds as a dermal substitute. *Burns* 2014;40:957-65. <https://doi.org/10.1016/j.burns.2013.09.026>
21. Mangera A, Bullock AJ, Roman S, et al. Comparison of candidate scaffolds for tissue engineering for stress urinary incontinence and pelvic organ prolapse repair. *BJU Int* 2013;112:674-85. <https://doi.org/10.1111/bju.12186>
22. Deshpande P, Ramachandran C, Sefat F, et al. Simplifying corneal surface regeneration using a biodegradable synthetic membrane and limbal tissue explants. *Biomaterials* 2013;34:5088-106. <https://doi.org/10.1016/j.biomaterials.2013.03.064>
23. Frazer J, Byea JB, Blacka L, et al. Development of bilayer and trilayer nanofibrous/microfibrous scaffolds for regenerative medicine. *Biomater Sci* 2013;1:942-51. <https://doi.org/10.1039/c3bm60074b>
24. Bye FJ, Bullock AJ, Singh R, et al. Development of a basement membrane substitute incorporated into an electrospun scaffold for 3D skin tissue engineering. *J Biomater Tissue Eng* 2014; 4: 686-92. <https://doi.org/10.1166/jbt.2014.1224>
25. Rheinwald JG, Green H. Serial cultivation of strains of human epidermal keratinocytes: The formation of keratinizing colonies from single cells. *Cell* 1975;6:331-43. [https://doi.org/10.1016/S0092-8674\(75\)80001-8](https://doi.org/10.1016/S0092-8674(75)80001-8)
26. Chapple C, Andrich D, Atala A, et al. SIU/ICUD Consultation on Urethral Strictures: The management of anterior urethral stricture disease using substitution urethroplasty. *Urology* 2014;83:S31-47. <https://doi.org/10.1016/j.urolgy.2013.09.012>
27. Wessells H, McAninch JW. Current controversies in anterior urethral stricture repair: Free-graft vs. pedicled skin-flap reconstruction. *World J Urol* 1998;16:175-80. <https://doi.org/10.1007/s003450050048>
28. Harrison CA, Gossiel F, Layton CM, et al. Use of an in vitro model of tissue-engineered skin to investigate the mechanism of skin graft contraction. *Tissue Eng* 2006;12:3119-33. <https://doi.org/10.1089/ten.2006.12.3119>
29. Patterson JM, Bullock AJ, MacNeil S, et al. Methods to reduce the contraction of tissue-engineered buccal mucosa for use in substitution urethroplasty. *Eur Urol* 2011;60:856-61. <https://doi.org/10.1016/j.eururo.2011.07.045>
30. Kulkarni RK, Pani KC, Neuman C, et al. Poly(lactic acid) for surgical implants. *Arch Surg* 1966;93:839-43.
31. Fu WJ, Zhang X, Zhang BH, et al. Biodegradable urethral stents seeded with autologous urethral epithelial cells in the treatment of post-traumatic urethral stricture: A feasibility study in a rabbit model. *BJU Int* 2009;104:263-8. <https://doi.org/10.1111/j.1464-410X.2009.08366.x>
32. Xu Y, Fu W, Wang Z, et al. A tissue-specific scaffold for tissue engineering-based ureteral reconstruction. *PLoS One* 2015;10:e0120244. <https://doi.org/10.1371/journal.pone.0120244>
33. Tong HW, Wang M, Li ZY, et al. Electrospinning, characterization and in vitro biological evaluation of nanocomposite fibers containing carbonated hydroxyapatite nanoparticles. *Biomed Mat* 2010;5:054111. <https://doi.org/10.1088/1748-6041/5/5/054111>
34. Bahari Javan N, Rezaie Shirmard L, Jafary Omid N, et al. Preparation, statistical optimisation, and in vitro characterisation of poly (3-hydroxybutyrate-co-3-hydroxyvalerate)/poly (lactic-co-glycolic acid) blend nanoparticles for prolonged delivery of teriparatide. *J Microencapsulation* 2016;1-15.
35. Li H, Chang J. Fabrication and characterization of bioactive wollastonite/PHBV composite scaffolds. *Biomaterials* 2004;25:5473-80. <https://doi.org/10.1016/j.biomaterials.2003.12.052>
36. Kose GT, Kokusuz F, Ozkul A et al. Tissue engineered cartilage on collagen and PHBV matrices. *Biomaterials* 2005 26:5187-97. <https://doi.org/10.1016/j.biomaterials.2005.01.037>
37. Li H, Chang J. Preparation, characterization and in vitro release of gentamicin from PHBV/wollastonite composite microspheres. *J Control Release* 2005;107:463-73. <https://doi.org/10.1016/j.jconrel.2005.05.019>
38. Ito Y, Hasuda H, Kamitakahara M, et al. A composite of hydroxyapatite with electrospun biodegradable nanofibers as a tissue engineering material. *J Biosci Bioeng* 2005;100:43-9. <https://doi.org/10.1263/jbb.100.43>
39. Yoon YI, Moon HS, Lyoo WS, et al. Superhydrophobicity of PHBV fibrous surface with bead-on-string structure. *J Colloid Interface Sci* 2008;320:91-5. <https://doi.org/10.1016/j.jcis.2008.01.029>
40. Li X, Liu KL, Wang M, et al. Improving hydrophilicity, mechanical properties and biocompatibility of poly[(R)-3-hydroxybutyrate-co-(R)-3-hydroxyvalerate] through blending with poly[(R)-3-hydroxybutyrate]-alt-poly(ethylene oxide). *Acta Biomaterialia* 2009;5:2002-12. <https://doi.org/10.1016/j.actbio.2009.01.035>
41. Wei G, Li C, Fu Q, et al. Preparation of PCL/silk fibroin/collagen electrospun fiber for urethral reconstruction. *Int Urol Nephrol* 2015;47:95-9. <https://doi.org/10.1007/s11255-014-0854-3>
42. Wang DJ, Li MY, Huang WT, et al. Repair of urethral defects with poly(lactid acid) fibrous membrane seeded with adipose-derived stem cells in a rabbit model. *Connect Tissue Res* 2015;56:434-9. <https://doi.org/10.1007/s0008207.2015.1035376>
43. Raya-Rivera A, Esquiliano DR, Yoo JJ, et al. Tissue-engineered autologous urethras for patients who need reconstruction: An observational study. *Lancet* 2011;377:1175-82. [https://doi.org/10.1016/S0140-6736\(10\)62354-9](https://doi.org/10.1016/S0140-6736(10)62354-9)

Correspondence: Dr. Abdulmuttalip Simsek, University of Sheffield, Department of Materials Science & Engineering, Sheffield, United Kingdom; simsek76@yahoo.com